



1 **The Probability Distribution of Daily Precipitation at the Point and**  
2 **Catchment Scales in the United States**

3  
4 Lei Ye<sup>1\*</sup>, Lars S. Hanson<sup>2</sup>, Pengqi Ding<sup>1</sup>, Dingbao Wang<sup>3</sup>, Richard M. Vogel<sup>4</sup>

5  
6 1 School of Hydraulic Engineering, Dalian University of Technology, Dalian, China

7 2 Institute for Public Research, Center for Naval Analyses, Arlington, Virginia, USA.

8 3 Department of Civil and Environmental Engineering, Tufts University, Medford, Massachusetts, USA

9 4 Department of Civil, Environmental, and Construction Engineering, University of Central Florida,  
10 Orlando, Florida, USA

11  
12 **Abstract:** Choosing a probability distribution to represent daily precipitation depths is  
13 important for precipitation frequency analysis, stochastic precipitation modeling and in  
14 climate trend assessments. Early studies identified the 2-parameter Gamma (G2)  
15 distribution as a suitable distribution for wet-day precipitation based on traditional  
16 goodness of fit tests. Here, probability plot correlation coefficients and L-moment  
17 diagrams are used to examine distributional alternatives for the full-record and wet-day  
18 series of daily precipitation at the point and catchment scales in the United States.  
19 Importantly, the G2 distribution performs poorly in comparison to either the Pearson  
20 Type-III (P3) or Kappa (KAP) distributions. The analysis indicates that the P3  
21 distribution fits the full record of daily precipitation at both the point and catchment  
22 scales remarkably well; while the KAP distribution best describes the distribution of wet-  
23 day precipitation at the point scale, and the performance of KAP and P3 distributions is  
24 comparable for wet-day precipitation at the catchment scale.

25  
26 **Key Words:** Climate; Rainfall; Weather; L-moment diagram; PPCC; Pearson type III;  
27 Kappa; Gamma; Wet-day; Frequency analysis; Trend detection; Stochastic weather  
28 models

29  
30 **1. Introduction**

31 Establishing a probability distribution that provides a good fit to daily  
32 precipitation depths has long been a topic interest in the fields of hydrology, meteorology,  
33 and others. The investigations into the daily precipitation distribution are primarily  
34 spread over three main research areas, namely, (1) stochastic precipitation models, (2)  
35 frequency analysis of precipitation, and (3) precipitation trends related to global climate  
36 change. Table 1 displays a sampling of the literature in these three fields, the particular  
37 precipitation series and durations under investigation, and the proposed distributions  
38 identified. Table 1 is by no means exhaustive; it only attempts to document the  
39 widespread interest in the determination of a suitable distribution for daily precipitation  
40 totals for various purposes.

41 *[Table 1 goes here]*

42 **1.1 Stochastic precipitation and climate models:**

---

\* Corresponding author. E-mail address: yelei@dlut.edu.cn



43           The first section in Table 1 presents a small portion of the literature related to  
44 stochastic precipitation modeling also referred to as stochastic weather modeling. The  
45 purpose of such models is not so much to investigate the properties of precipitation, but  
46 instead to produce artificially generated precipitation sequences that can be used as inputs  
47 to other models to explore the behavior of hydrologic systems (Buishand, 1978;Waymire  
48 and Gupta, 1981). A wide range of types of stochastic precipitation generators exist as  
49 evidenced from review articles Waymire and Gupta (1981), Wilks and Wilby (1999),  
50 Srikanthan and McMahon (2001) and Chen and Brissette (2014). Also see the  
51 introduction of Mehrotra et al. (2006) for a nice review.

52           Since our central goal is to select a suitable generalized probability distribution  
53 for modeling daily precipitation depths, we are only concerned with the class of “two-  
54 part” stochastic daily precipitation models that utilize a probability distribution function  
55 to describe precipitation amounts on wet-days, while precipitation occurrence is  
56 separately described using a Markov model or some form of a stochastic renewal process  
57 (Buishand, 1978;Geng et al., 1986;Waymire and Gupta, 1981;Watterson, 2005).

58           It is evident from Table 1 that the wet-day precipitation series is virtually the only  
59 daily precipitation series that is even considered in the stochastic precipitation model  
60 literature. Thom’s (1951) suggestion of the 2-parameter Gamma (G2) distribution  
61 function for wet-day amounts seems to carry considerable weight. Following the  
62 suggestion of numerous previous authors, both Watterson and Dix (2003) and Watterson  
63 (2005) assumed a Gamma distribution for wet-day rainfall in the development of  
64 stochastic rainfall models.. Buishand (1978) lent support to the suggestion of the Gamma  
65 distribution by showing that for the wet-day series at six stations, the empirical  
66 Coefficient of Variation to Coefficient of Skewness ratio was quite close to the  
67 theoretical value of two for a Gamma distribution.

68           Geng et al. (1986) used a simple regression to show that the beta parameter of the  
69 Gamma distribution for a given month can be predicted reasonably well by the average  
70 rainfall per wet-day in that month. Geng et al. (1986) also provided a good review of  
71 other literature supporting the use of the Gamma distribution for modeling wet-day  
72 rainfall.

73           While the G2 distribution is by far the most preferred distribution for wet-day  
74 precipitation amounts, other distributions have also been suggested. Woolhiser and  
75 Roldan (1982) and Wilks (1998) both suggested the use of a three-parameter mixed  
76 exponential distribution instead of G2. The three-parameter exponential distribution can  
77 describe wet-day amounts by mixing two distinct exponential distributions (each with its  
78 own mean parameter) with a parameter that chooses which one to use. Through a variety  
79 of goodness of fit tests and log-likelihood analyses, the mixed exponential is shown as  
80 being preferred to G2 (Wilks, 1998).

81           The Weibull (W2) and to a lesser extent the exponential distribution have also  
82 been suggested for modeling daily precipitation amounts (Duan et al., 1995;Burgueno et  
83 al., 2005). Duan et al. (1995) used a Chi-squared test to demonstrate that synthetic  
84 rainfall generated from the Weibull and Gamma (with parameters estimated by method of  
85 moments) models best matches the observed data within each month. Separate models



86 were created for each calendar month. (Burgueno et al., 2005) used graphical methods  
87 and the Kolmogorov-Smirnov test to give support to the W2 and exponential distributions.

## 88 **1.2 Precipitation frequency analysis:**

89 The second section of Table 1 displays a small portion of the literature related to  
90 precipitation frequency analyses. Extreme values of rainfall are of particular interest to  
91 urban planners, engineers and hydrologists working on problems related to storm  
92 drainage, flooding, and other natural hazards such as precipitation-induced slope failures  
93 (landslides). Precipitation frequency analyses are one way to generate the necessary  
94 precipitation totals at given return period for hydraulic design purposes. A key step in  
95 frequency analysis of precipitation involves selection of a suitable distribution for  
96 representing precipitation depths to investigate the extremes. While these analyses can  
97 be conducted for multiple precipitation durations, we focus on those that investigate the  
98 1-day duration.

99 As the extreme rainfall values are of primary importance in these studies, a highly  
100 censored series of rainfall is often useful in these analyses. The Annual Maximum Series  
101 (AMS) and Partial Duration Series (PDS) are often used in hydrologic frequency  
102 investigations (Stedinger et al., 1993). Table 1 displays that many of the precipitation  
103 frequency investigations of daily precipitation depths have selected the AMS series. The  
104 wet-day series is actually a PDS with zeros and values lower than the detection limit of  
105 the instrument (i.e., “trace” values) censored.

106 In perhaps the most comprehensive assessment of the distribution of precipitation  
107 extremes, Papalexioiu and Koutsoyiannis (2013) examined the goodness-of-fit of the  
108 GEV distribution to a global dataset of AMS at 15,137 sites with lengths varying from 40  
109 to 163 years. Analysis of such a large dataset enabled them to conclude that GEV models  
110 of AMS series of daily precipitation provide a good approximation with the shape  
111 parameter depending critically upon both the location and length of the series under  
112 consideration. Interestingly, when record length and location are taken into account, the  
113 shape parameter appears to exhibit a relatively narrow range of small positive values.

114 For many years, the most common approach to summarizing precipitation  
115 frequency analyses in the United States was the work of Hershfield (1961), which is  
116 commonly referred to as TP-40. Hershfield (1961) fitted a Gumbel distribution to the  
117 AMS series of 24-hour precipitation. More recently investigators have completed these  
118 types of analyses by using the method of L-moments and other methods that are more  
119 powerful than the traditional goodness of fit measures. In the context of a national  
120 revision to the TP-40 rainfall frequency atlas and after the application of L-moment  
121 goodness-of-fit evaluations, Bonnin et al., (2006) fitted a generalized extreme value  
122 (GEV) distribution to the AMS of rainfall.

123 Bonnin et al. (2006) performed a very comprehensive national assessment of  
124 precipitation frequency by applying the most up-to-date developments in regional  
125 frequency analysis to series of annual maximum n-minute precipitation. Using both at-  
126 site and regional L-moment goodness-of-fit results, climatic considerations and  
127 sensitivity testing, the GEV distribution was selected to best represent the underlying  
128 distributions of all daily and hourly AMS rainfall data. GEV was also selected for the 5-  
129 10-, and 15-minute AMS rainfall data. Naghavi and Yu (1995) also chose the GEV for a



130 study of rainfall extremes in Louisiana. Similarly, Lee and Maeng (2003) selected the  
131 GEV and the generalized logistic distributions based on L-moment analysis of 58 stations  
132 in Korea.

133 While the results of Bonnin et al. (2006) apply to the United States, other authors  
134 have found similar results using similar methods in other parts of the world. Pilon et al.  
135 (1991) used L-moment goodness-of-fit results to show that the Gumbel distribution  
136 should be rejected in the favor of the GEV in Ontario, Canada. In Korea, Park and Jung  
137 (2002) successfully used the Kappa distribution (of which the GEV is a special case) to  
138 generate extreme precipitation quantile maps using both Maximum Likelihood  
139 Estimators (MLE) and L-moment estimators (L-ME) for Kappa parameter estimation.  
140 They found convergence failure at some stations for the L-ME, and lack of fit for those  
141 series fit with MLEs when sample size was too small.

142 Interestingly, while a great deal of attention is given to fitting distributions to the  
143 relatively short AMS series of precipitation depths, very few studies directly explore the  
144 probability distribution of the complete series of daily precipitation (including zeros) or  
145 the wet-day series of daily precipitation (zeros excluded). Shoji and Kitaura (2006)  
146 investigated both full-record and wet-day daily precipitation series, but included only the  
147 normal, lognormal, exponential, and Weibull distributions as candidate distributions, and  
148 did not employ modern regional hydrologic methods such as the method of L-moments.

149 Perhaps the most thorough investigations, to date, on the probability distribution  
150 of daily precipitation amounts are the global studies by Papalexiou and Koutsoyiannis  
151 (2012, 2016). Papalexiou and Koutsoyiannis (2012) derived a generalized Gamma  
152 distribution (GG) from Entropy theory, using plausible constraints for wet-day series of  
153 daily precipitation series. Together, the two studies by Papalexiou and Koutsoyiannis  
154 (2012, 2016) revealed that the GG distribution provides a good approximation to the  
155 behavior of observed L-moments of global series of wet-day daily precipitation at 11,519  
156 and 14,157 stations, respectively.

157 Deidda and Puliga (2006) investigated the degree of left-censoring of wet-day  
158 series needed to fit a Generalized Pareto (GPA) distribution for 200 stations in Sardinia,  
159 Italy with a range of modern statistical analysis techniques. The “failure-to-reject”  
160 goodness-of-fit method was used to establish an optimal threshold for left censoring at  
161 each station to make the observed data fit a GPA distribution. Often, Deidda and Puliga  
162 (2006) found that no optimal threshold for left censoring could make the data fit a GPA  
163 distribution at 5 and 10% confidence intervals. Deidda and Puliga (2006) remarked that  
164 data rounding off may explain some of the lack of fit, but their results still leave room for  
165 debate on the most likely candidate distribution for daily precipitation.

### 166 **1.3 Precipitation trends and changes:**

167 The third section of Table 1 summarizes a small portion of the precipitation trend  
168 literature which has become a rather large area of inquiry due to concerns over climate  
169 change, as evidenced from recent reviews on the subject (Easterling et al.,  
170 2000; Trenberth, 2011; Madsen et al., 2014). Interestingly, within the literature devoted to  
171 detection of changes in precipitation patterns, we find a reliance on previous studies of  
172 the probability distribution of daily precipitation for evaluating changes in distributional  
173 parameters and in selecting candidate distributions. Almost universally, the G2



174 distribution appears to be accepted without serious consideration of alternative  
175 distributions. For instance, (Groisman et al., 1999) wrote simply, “It is widely  
176 recognized that the distribution of daily precipitation totals,  $P$ , can be approximated by  
177 the Gamma distribution.” That is not to say the G2 distribution is not tested for its fit to  
178 the observed data. For instance, (Groisman et al., 1999) compared maps of the empirical  
179 probability of summer 1-day rainfall exceeding 50.4 mm with maps of probabilities  
180 determined by a stochastic model using the fitted G2 distribution for the amounts. They  
181 found acceptable fits in regions where there are enough observed daily rainfall events  
182 greater than 50.4 mm.

183 This is an interesting contrast to the precipitation frequency analysis literature  
184 where a Gamma distribution is often fit to wet-day series for the purpose of examining  
185 extreme rainfalls instead of using the AMS series fitted by a GEV or other distribution.  
186 Yoo et al. (2005) explained that conventional frequency analysis (using AMS) cannot  
187 expect to predict precipitation changes resulting from climate change; while an  
188 examination of the differences in the Gamma distribution’s parameters (fitted to the  
189 whole wet-day record) might predict such changes. They found that modifying the  
190 parameters of the daily Gamma distribution can explain changes in rainfall quantiles  
191 predicted by General Circulation Models (GCM) under various climate change scenarios.  
192 Wilby and Wigley (2002) plotted the expected 100-year changes in the shape and scale  
193 parameter of the G2 distribution according to two GCM models’ predictions.

194 In a national study of precipitation trends, Karl and Knight (1998) employed the  
195 G2 distribution to fill in missing precipitation observations. Karl and Knight (1998) wrote  
196 that “To determine if precipitation occurs on any missing day, a random number  
197 generator is used such that the probability of precipitation is set equal to the empirical  
198 probability of precipitation during that month. If precipitation occurs, then the gamma  
199 distribution is used to determine the amount that falls for that day, again using a random  
200 number generator.” Both Watterson and Dix (2003) and Watterson (2005) assumed a G2  
201 distribution for daily precipitation in the development of stochastic rainfall models for  
202 use in evaluating changes in precipitation extremes.

203 We conclude from this brief review that both the precipitation trend and climate  
204 change literature have widely used the G2 distribution as a powerful tool to examine not  
205 only the possible changes in precipitation patterns, but also the relative rate of change in a  
206 geospatial context through mapping. In summary, there are a wide variety of previous  
207 studies which have explored the probability distribution of daily precipitation for the  
208 purposes of precipitation frequency analysis, stochastic precipitation modeling and for  
209 trend detection. There seems to be a consensus that annual maxima appear to be well  
210 approximated by either a GEV, Gumbel or Gamma probability density function (pdf) and  
211 that series of wet-day daily precipitation totals are well approximated by a Gamma  
212 Generalized Gamma, or in some cases a mixed exponential pdf. However, other than the  
213 two recent global studies by Papalexou and Koutsoyiannis (2012, 2016). We are  
214 unaware of any studies that have used recent developments in regional hydrologic  
215 frequency analysis such as L-moment diagrams or probability plot goodness of fit  
216 evaluations to evaluate the probability distribution of the *complete series* of daily  
217 precipitation.



218 The recent studies by Papalexiou and Koutsoyiannis (2012, 2016) represent  
219 perhaps the most comprehensive studies to date, however, they only consider wet-day  
220 series of daily precipitation and their L-moment evaluations only evaluate the  
221 relationship between L-Skewness and L-Cv, thus they were unable to fully evaluate the  
222 goodness-of-fit of the several relatively new three-parameter pdfs introduced in their  
223 studies such as the generalized Gamma (GG) and the generalized Burr type XII (GB)  
224 pdfs which would require construction of L-Kurtosis versus L-Skew diagrams.  
225 Analogous to those two studies, this paper uses several large scale national datasets to re-  
226 examine the question of which of the commonly used continuous distribution functions  
227 which are widely used in the fields of hydrology, meteorology and climate best fit both  
228 wet-day and complete series of observed daily precipitation data.

229 Instead of considering the GG distribution, the pdf recommended by both  
230 Papalexiou and Koutsoyiannis (2012, 2016), which is only suited to wet-day series, has  
231 seen very limited use and for which analytical and/or polynomial relationships for L-  
232 Kurtosis are unavailable as they are for most commonly used pdfs in hydrology, we  
233 consider the more widely used 3 parameter generalization of the Gamma distribution  
234 known as the Pearson type III (P3) distribution. Once analytical and polynomial L-  
235 moment relationships and parameter estimation methods become available for the GG  
236 distribution, future studies should compare the P3 and GG distributions on wet-day series,  
237 because on the basis of this study, and Papalexiou and Koutsoyiannis (2016), the P3 and  
238 GG distributions appear to have tremendous potential for approximating the distribution  
239 of wet-day series.

240 Our primary objective is to use a very large spatially distributed dataset at both  
241 the point and catchment scales, to determine a suitable probability distribution of full-  
242 record series and wet-day series of daily precipitation using L-moment diagrams and  
243 probability plot correlation coefficient goodness of fit statistics. Analogous to the recent  
244 study by Papalexiou and Koutsoyiannis (2016), these evaluations yield very different  
245 conclusions than previous research on this subject.

## 246 **2. Study area and data**

247 Precipitation depths at the point and catchment scales are important information  
248 in hydrology, meteorology, and other fields, thus our study focuses on both of them. For  
249 point precipitation, we employ a data set comprised of daily precipitation depths at 237  
250 first-order NOAA stations from 49 U.S. states (Hawaii is excluded due to fundamentally  
251 different precipitation behavior). Station locations are shown in Figure 1a. In contrast,  
252 the areal average precipitation for 305 catchments in the international Model Parameter  
253 Estimation Experiment (MOPEX) data set (Duan et al., 2006) is also selected for analysis.  
254 The catchment locations and boundaries are shown in Figure 1b. The data were quality  
255 controlled to remove null values. When greater than 6 null values occurred in a given  
256 year or greater than 3 in a given month, the full year of data was removed. When fewer  
257 than these numbers of null values were present, they were treated as zeroes. The average  
258 record length for point precipitation depths for the 237 sites is 24,657 days (67.5 years).  
259 The distribution of record lengths corresponding to the 237 first-order NOAA stations is  
260 shown in Figure 2. The MOPEX data set consists of 56 years of areal average



261 precipitation from 1948 to 2003, corresponding to a fixed record length 20,454 days for  
262 each of the 305 catchments shown in Figure 1b.

263 *[Figure 1 goes here]*

264 *[Figure 2 goes here]*

265 In addition to the full-record series of daily precipitation, wet-day series were  
266 extracted from both data sets. The wet-day series were constructed by excluding zero  
267 and “trace” values (those with less than “0.01” recordable precipitation). Wilks (1990)  
268 discussed other ways to treat trace precipitation and left-censored data, but for  
269 convenience, they are simply excluded. The mean wet-day record lengths for point and  
270 areal average precipitation are 7,219 days (equivalent to nearly 20 years) and 14,043 days  
271 (more than 38 years), respectively. The distributions of wet-day record length are shown  
272 in Figure 3. As expected, the proportion of wet-days in the areal average precipitation  
273 data set is higher than that in the point precipitation data set.

274 *[Figure 3 goes here]*

### 275 **3. Methodology**

276 This section describes the methods of analysis used for assessing the goodness-of-  
277 fit of various distributional hypotheses, namely, L-moment diagrams and probability plot  
278 correlation coefficients.

#### 279 **3.1 L-Moment Diagrams**

280 L-moment diagrams are now a widely accepted approach for evaluating the  
281 goodness of fit of alternative distributions to observations. The theory and application of  
282 L-moments introduced by Hosking (1990) is now widely available in the literature  
283 (Stedinger et al., 1993; Hosking and Wallis, 1997), hence it is not reproduced here.

284 The distribution of daily precipitation totals is highly skewed due to the large  
285 proportion of days with zero precipitation. Higher order conventional moment ratios such  
286 as skewness and kurtosis are very sensitive to extreme values and can exhibit enormous  
287 downward bias even for extremely large sample sizes (Vogel and Fennessey, 1993) as is  
288 the case here. However, L-moment ratios are approximately unbiased in comparison to  
289 conventional moment ratios, thus providing a particularly useful tool for investigating the  
290 pdf of precipitation series.

291 L-moment ratio diagrams provide a convenient visual way to view the  
292 characteristics of sample data compared to theoretical statistical distributions. The L-  
293 moment diagrams: L-Kurtosis ( $\tau_4$ ) vs L-Skew ( $\tau_3$ ) and L-Cv ( $\tau_2$ ) vs L-Skew ( $\tau_3$ ) enable us  
294 to compare the goodness of fit of a range of three-parameter, two-parameter, and one-  
295 parameter (or special case) distributions. Table 2 displays distributions analyzed by  
296 means of the  $\tau_4$  vs  $\tau_3$  L-moment ratio diagrams.

297 *[Table 2 goes here]*

298 Table 3 displays distributions analyzed by means of the  $\tau_2$  vs  $\tau_3$  L-moment ratio  
299 diagrams.

300 *[Table 3 goes here]*



301 L-moment ratio diagrams have been used before to examine the distribution of  
302 series of annual maximum precipitation data (Pilon et al., 1991; Park and Jung, 2002; Lee  
303 and Maeng, 2003; Papalexiou and Koutsoyiannis, 2013) and left-censored records  
304 (Deidda and Puliga, 2006). Other than the two recent global studies by Papalexiou and  
305 Koutsoyiannis (2012, 2016) which examined the agreement between empirical and  
306 theoretical relationships between L-Cv and L-Skew, this is the only study we are aware  
307 of, in which a set of uncensored daily precipitation records have been subjected to such a  
308 comprehensive L-moment goodness-of-fit analysis. L-moment estimators were chosen in  
309 this study for a variety of reasons: (1) they are easily computed and nicely summarized  
310 by Hosking and Wallis (1997) for all the cases considered in this study, and (2) estimates  
311 of L-moments unbiased and estimates of their ratios are nearly unbiased, and thus for the  
312 extremely large sample sizes considered here, sampling variability of empirical L-  
313 moment ratios will be extremely small especially when contrasted to distributional choice  
314 comparisons.

### 315 **3.2 Probability plot correlation coefficient goodness-of-fit evaluation**

316 Probability plots are constructed for each of the full record and wet-day series  
317 using L-moment estimators of the distribution parameters (see Hosking and Wallis  
318 (1997)) for the distributions indicated in Table 4.

319 *[Table 4 goes here]*

320 The goodness of fit of each probability plot is summarized using a probability plot  
321 correlation coefficient (PPCC, or simply,  $r$ ). The PPCC statistic has a maximum value of  
322 1. The PPCC has been shown to be a powerful statistic for evaluating the goodness-of-fit  
323 of a very wide range of alternative distributional hypotheses (Stedinger et al., 1993) and  
324 for performing hypothesis tests of various two parameter distributional alternatives.

325 To construct a probability plot and to estimate a probability plot correlation  
326 coefficient, requires estimation of a plotting position. There are two classes of plotting  
327 positions, those that yield unbiased exceedance probabilities and those that yield unbiased  
328 quantile estimates. The Weibull plotting position given by  $p=i/(n+1)$  yields an unbiased  
329 estimate of exceedance probability regardless of the underlying distribution (see  
330 (Stedinger et al., 1993)). Alternatively there would be a unique plotting position to use  
331 for each probability distribution, and it is now well known that unbiased plotting  
332 positions for three parameter distributions require an additional parameter to estimate  
333 within the plotting position. For example, Vogel and McMartin (1991) derived an  
334 unbiased plotting position for the P3 distribution which depends upon the skewness of the  
335 distribution, a parameter which adds so much additional uncertainty to the analysis that  
336 led Vogel and McMartin (1991), after considerable analysis, to not recommend its use.  
337 To put all the distributional alternatives on the same footing, we chose to use the Weibull  
338 plotting position for estimation of all PPCC values.

## 339 **4. Results and analysis**

### 340 **4.1 L-Moment Diagrams**

#### 341 **4.1.1 L-Cv vs L-Skew**





342 Figure 4 displays empirical and theoretical distributional relationships between L-  
343 Cv and L-Skew for point values of daily precipitation (Figure 4a) and areal average  
344 values of daily precipitation (Figure 4b). The various curves represent the theoretical  
345 relationship between L-Cv and L-Skew for the distributions indicated. Each plotted point  
346 represents the empirical relationship between L-Cv and L-Skew for a single precipitation  
347 station or catchment. By comparing the empirically derived points with the theoretical  
348 curves, it is possible to see the degree to which the statistical character of the data record  
349 matches those of the candidate distributions. We emphasize again, that the sample sizes  
350 are large enough in this study so that one may, approximately, ignore sampling variability  
351 in all L-moment diagrams. This phenomenon was nicely illustrated in Figure 2 of Blum  
352 et al. (2017) for record lengths similar to those used here, but corresponding to daily  
353 streamflow records.

354 The empirical L-moment ratios corresponding to the full-record and wet-day point  
355 precipitation series fall within completely different regions in Figure 4a, which is due to  
356 the fact that the full-record point precipitation series contain a very large number of zero  
357 observations. In contrast, there are much fewer zero observations in the catchment full-  
358 record precipitation series thus the empirical L-moment ratios corresponding to the full-  
359 record and wet-day catchment precipitation series overlap roughly 50% of the time as  
360 shown in Figure 4b.

361 Both Figure 4a and Figure 4b illustrate a nearly linear relationship between the L-  
362 Skew and L-Cv for the two types of full record series. Importantly, these two lines of  
363 points, however, do not fall along any of the theoretical curves, demonstrating that the 2-  
364 parameter Gamma distribution cannot describe the tail behavior of full-record series of  
365 precipitation as has often been assumed in the past.

366 *[Figure 4 goes here]*

367 In Figure 4a, the wet-day series' points fall primarily within a region bounded by  
368 the G2 and GP2 theoretical curves, with the W2 passing through some of the points. In  
369 Figure 4b, the wet-day series' points fall primarily in the upper region of the W2  
370 theoretical curve, with the G2 passing through some of the points. These patterns do not  
371 indicate a clearly preferred distribution, especially considering that the large sample sizes  
372 associated with these series result in negligible sampling variability. Blum et al. (2017,  
373 Figure 2) used L-moment diagrams for complete series of daily streamflow observations  
374 to demonstrate that the sampling variability in L-moment ratios is negligible for the  
375 sample sizes considered in this study. Thus, the scatter shown in Figure 4 is likely due to  
376 real distributional differences rather than due to sampling variability as is often the case  
377 when one constructs L-moment diagrams for short AMS precipitation records.

#### 378 4.1.2 L-Kurtosis vs L-Skew

379 Figure 5 displays empirical and theoretical distributional relationships between L-  
380 Kurtosis vs L-Skew point values of daily precipitation (Figure 5a) and areal average  
381 values of daily precipitation (Figure 5b). The plotted points for the two full record series  
382 follow a linear relationship approximately, but the relationships are remarkably similar to  
383 the theoretical curve for the Pearson Type-III (P3) distribution. In fact, the P3 pdf seems  
384 to be the only 3-parameter distribution that could possibly fit the full record data. It is



385 worth noting that the overall lower bound of L-Kurtosis for all distributions falls below  
386 but quite close to the P3 curve at high L-Skew values in Figure 5.

387 *[Figure 5 goes here]*

388 The estimated L-moment ratios of the wet-day series of point precipitation in  
389 Figure 5a reveal more scatter on the plot than for the corresponding full-record series. In  
390 this case, the closest theoretical curve to the wet-day points is also the P3 distribution, but  
391 the fit is less striking for the wet-day series than for the corresponding full record series.  
392 In Figure 5b, the L-moment ratios of the wet-day series of areal average precipitation  
393 shows less scatter than for the corresponding full record series and in this case of areal  
394 rainfall the P3 theoretical curve passes through most of the points for both the full and  
395 wet-day series. Though the fit of the wet-day series to P3 is less striking than for the full  
396 record series, the L-moment ratio estimates occupy a space that can be well represented  
397 by the Kappa distribution, which occupies not a curve, but a region of the L-Kurtosis vs  
398 L-Skew diagram as shown in Figure A1 of Hosking and Wallis (1997). See Hosking  
399 (1994) and Hosking and Wallis (1997, Appendix A10) for a complete description of the  
400 4-parameter Kappa distribution.

## 401 **4.2 PPCC**

### 402 **4.2.1 Standard boxplots of PPCC**

403 The L-moment diagrams successfully identify two potential candidate  
404 distributions for representing the full-record and wet-day daily precipitation series at the  
405 point and catchment scales. The PPCC statistic offers another quantitative method for  
406 comparing the goodness of fit of different distributions to the daily precipitation  
407 observations. Tables 5 and 6 summarize the central tendency and spread of the values of  
408 PPCC for each of the distributions for both the full-record and wet-day series of point and  
409 catchment scale daily precipitation, respectively. The highest values for the mean,  
410 median, 95<sup>th</sup> percentile, and 5<sup>th</sup> percentile of the PPCC are shown in bold type. The  
411 lowest values of the sample standard deviation of the PPCC values, denoted  $\hat{s}$ , are also  
412 shown in bold. Figure 6 illustrates box-plots of the values of PPCC for distributions  
413 fitted to the full-record and wet-day series of daily precipitation data at the point scale.  
414 Figure 7 shows box-plots of PPCC values for distributions fitted to the full-record and  
415 wet-day precipitation series at the catchment scale.

416 *[Table 5 goes here]*

417 *[Table 6 goes here]*

418 *[Figure 6 goes here]*

419 *[Figure 7 goes here]*

420 Figure 6 and Table 5 indicate that for the full-record series of point daily  
421 precipitation depths, only the G2, P3, and KAP distributions perform well. On the other  
422 hand, for the wet-day series of point daily precipitation, all the distributions have median  
423 PPCCs well above 0.9. The same situation appears in the areal average precipitation  
424 shown in Figure 7 and Table 6, except that the median PPCCs of the remaining four  
425 distributions for the wet-day series are significantly lower than the corresponding values  
426 for point precipitation.



427 The insets in Figures 6 and 7 show detailed views of the boxplots of PPCC values  
428 for the G2, P3, and KAP distributions for point and areal average daily precipitation.  
429 Both types of precipitation data shows the same results that the P3 is the best performing  
430 distribution on average for the full-record series, but the KAP distribution shows the  
431 highest PPCCs on average for the wet-day series.

#### 432 **4.2.2 Graphical comparison of P3, G2, and KAP**

433 Across all previous comparison, the P3, G2, and KAP are the most likely  
434 distributions for describing daily precipitation at the point or catchment scales. The  
435 insets in Figures 6 and 7 identify the distributions that exhibit the best fit to the observed  
436 series. However, these inserts do not indicate by how much the best performing  
437 distribution outperforms the second or third best. For this purpose, pairwise comparisons  
438 of the PPCC values of two highly performing distributions for all the stations and  
439 catchments are instructive. A simple graphical method can accomplish this goal.

440 Figure 8a and Figure 8b compare the PPCC values of the P3 (vertical axis) and  
441 G2 (horizontal axis) distributions for the full-record and wet-day series of point daily  
442 precipitation, respectively. Approximately 98% of stations are displayed on both figures;  
443 the remaining stations lie outside the plot domains. Points lying above the diagonal line  
444 indicate that the P3 distribution has a higher PPCC for that particular station, and points  
445 lying below the diagonal line indicate the G2 results in a higher PPCC. The full-record  
446 plot (Figure 8a) shows that in nearly every case, the P3 distribution outperforms the G2  
447 distribution. When the G2 does outperform the P3, the PPCCs are both very high and  
448 nearly equal. The wet-day plot shows that the P3 distribution performs significantly  
449 better than the G2 distribution in many cases. Thus, we conclude the P3 distribution  
450 better represents wet-day daily point precipitation than the more commonly used G2  
451 distribution, in nearly every case.

452 *[Figure 8 goes here]*

453 Figures 8c and Figure 8d compare the PPCC values of P3 and G2 for the full  
454 record series and wet-day series of areal average precipitation, respectively. The results  
455 are nearly the same as for the point precipitation in the sense that most points are above  
456 the diagonal line; while for a few catchments when G2 does outperform P3, the points lie  
457 on the dividing line, showing only very slight superiority.

458 Figure 9a and Figure 9b display similar plots comparing the KAP (vertical axis)  
459 and P3 (horizontal axis) distribution, for the full-record and wet-day series of point  
460 precipitation, respectively. For the full-record series the P3 distribution outperforms the  
461 KAP distribution with most of the points lying below the dividing line; whereas, for the  
462 wet-day series, the KAP distribution outperforms the P3 distribution for a majority of  
463 sites.

464 *[Figure 9 goes here]*

465 The same conclusion can be obtained for the full-record series of areal average  
466 precipitation in Figures 9c except that the better distribution does not dominate, with only  
467 63% points have higher PPCC for P3 distributions. For the wet-day series of areal  
468 average precipitation in Figures 9d, the performance of KAP distribution is comparable  
469 with that of P3 distribution with almost the same number of points lying in each region.



470 It is somewhat surprising that the 3-parameter P3 distribution outperforms the 4-  
471 parameter KAP distribution because the extra information contained in the 4<sup>th</sup> parameter  
472 (essentially a second shape parameter in the case of the Kappa distribution) would be  
473 expected to lead to a better goodness-of-fit. The L-moment diagram (Figure 5), however,  
474 shows that the fit of the full record data to the P3 theoretical curve is so good that a 4<sup>th</sup>  
475 parameter could be extraneous. Additionally, it should be noted that the pattern of the  
476 full record stations or watersheds on the L-Kurtosis vs L-Skew plot approaches the  
477 overall lower bound for all distributions, a place where the Kappa distribution parameter  
478 estimates may become less accurate. The “h” shape parameter, for example, approaches  
479 infinity in this region (see Hosking and Wallis (1997, Figure A1)).

## 480 5. Conclusions

481 This study has demonstrated that L-moment diagrams and probability plot  
482 correlation coefficient goodness of fit evaluations can provide new insight into the  
483 distribution of very long series of daily precipitation at both the point and catchment  
484 scales. Though the commonly used 2-parameter Gamma distribution performs fairly well  
485 on the basis of traditional goodness-of-fit tests, L-moment diagrams and probability plot  
486 correlation coefficient goodness of fit evaluations reveal that very long series of  
487 uncensored daily point and areal average precipitation are better approximated by a  
488 Pearson-III distribution and importantly, they do not resemble any of the other commonly  
489 used distributions.

490 We conclude that for representing uncensored, full record daily precipitation at  
491 the point and catchment scales, the 3-parameter Pearson-III distribution performs  
492 remarkably well. For cases in which only wet-day precipitation amounts are required, the  
493 Pearson-III distribution is comparable with the 4-parameter Kappa distribution for the  
494 areal average precipitation; when the point precipitation is of concern, the Kappa  
495 distribution should be the distribution of choice. We also conclude that future  
496 investigations should consider comparisons between the generalized Gamma distribution  
497 introduced by Papalexiou and Koutsoyiannis (2012, 2016) for wet-day daily precipitation  
498 and both the Pearson type III and Kappa distributions recommended here.

## 499 Acknowledgements

500 This work is partially supported by the National Natural Science Foundation of China  
501 (No. 91547116, 51709033, 91647201).  
502

## 503 References

- 504 Blum, A. G., Archfield, S. A., and Vogel, R. M.: On the probability distribution of daily  
505 streamflow in the United States, *Hydrology and Earth System Sciences*, 21, 3093, 2017.
- 506 Bonnin, G. M., Martin, D., Lin, B., Parzybok, T., Yekta, M., and Riley, D.: Precipitation-  
507 frequency atlas of the United States, NOAA atlas, 14, 2006.
- 508 Buishand, T. A.: Some remarks on the use of daily rainfall models, *Journal of Hydrology*,  
509 36, 295-308, 1978.



- 510 Burgueno, A., Martinez, M. D., Lana, X., and Serra, C.: Statistical distributions of the  
511 daily rainfall regime in Catalonia (northeastern Spain) for the years 1950–2000,  
512 *International Journal of Climatology*, 25, 1381–1403, 2005.
- 513 Chen, J., and Brissette, F. P.: Stochastic generation of daily precipitation amounts: review  
514 and evaluation of different models, *Climate Research*, 59, 189–206, 2014.
- 515 Deidda, R., and Puliga, M.: Sensitivity of goodness-of-fit statistics to rainfall data  
516 rounding off, *Physics and Chemistry of the Earth, Parts A/B/C*, 31, 1240–1251, 2006.
- 517 Duan, J., Sikka, A. K., and Grant, G. E.: A comparison of stochastic models for  
518 generating daily precipitation at the HJ Andrews Experimental Forest, 1995.
- 519 Duan, Q., Schaake, J., Andreassian, V., Franks, S., Goteti, G., Gupta, H. V., Gusev, Y.  
520 M., Habets, F., Hall, A., and Hay, L.: Model Parameter Estimation Experiment (MOPEX):  
521 An overview of science strategy and major results from the second and third workshops,  
522 *Journal of Hydrology*, 320, 3–17, 2006.
- 523 Easterling, D. R., Evans, J., Groisman, P. Y., Karl, T. R., Kunkel, K. E., and Ambenje, P.:  
524 Observed variability and trends in extreme climate events: a brief review, *Bulletin of the*  
525 *American Meteorological Society*, 81, 417–425, 2000.
- 526 Geng, S., de Vries, F. W. P., and Supit, I.: A simple method for generating daily rainfall  
527 data, *Agricultural and Forest Meteorology*, 36, 363–376, 1986.
- 528 Groisman, P. Y., Karl, T. R., Easterling, D. R., Knight, R. W., Jamason, P. F., Hennessy,  
529 K. J., Suppiah, R., Page, C. M., Wibig, J., and Fortuniak, K.: Changes in the probability  
530 of heavy precipitation: important indicators of climatic change, in: *Weather and Climate*  
531 *Extremes*, Springer, 243–283, 1999.
- 532 Hershfield, D. M.: Rainfall frequency atlas of the United States for durations from 30  
533 minutes to 24 hours and return periods from 1 to 100 years, 1961.
- 534 Hosking, J. R.: L-moments: analysis and estimation of distributions using linear  
535 combinations of order statistics, *Journal of the Royal Statistical Society. Series B*  
536 (Methodological), 105–124, 1990.
- 537 Hosking, J. R.: The four-parameter kappa distribution, *IBM Journal of Research and*  
538 *Development*, 38, 251–258, 1994.
- 539 Hosking, J. R. M., and Wallis, J. R.: *Regional frequency analysis: an approach based on*  
540 *L-moments*, Cambridge University Press, 1997.
- 541 Karl, T. R., and Knight, R. W.: Secular trends of precipitation amount, frequency, and  
542 intensity in the United States, *Bulletin of the American Meteorological Society*, 79, 231–  
543 241, 1998.
- 544 Lee, S. H., and Maeng, S. J.: Frequency analysis of extreme rainfall using L moment,  
545 *Irrigation and Drainage*, 52, 219–230, 2003.
- 546 Madsen, H., Lawrence, D., Lang, M., Martinkova, M., and Kjeldsen, T.: Review of trend  
547 analysis and climate change projections of extreme precipitation and floods in Europe,  
548 *Journal of Hydrology*, 519, 3634–3650, 2014.



- 549 Mehrotra, R., Srikanthan, R., and Sharma, A.: A comparison of three stochastic multi-site  
550 precipitation occurrence generators, *Journal of Hydrology*, 331, 280-292, 2006.
- 551 Naghavi, B., and Yu, F. X.: Regional frequency analysis of extreme precipitation in  
552 Louisiana, *Journal of Hydraulic Engineering*, 121, 819-827, 1995.
- 553 Papalexiou, S. M., and Koutsoyiannis, D.: Entropy based derivation of probability  
554 distributions: A case study to daily rainfall, *Advances in Water Resources*, 45, 51-57,  
555 2012.
- 556 Papalexiou, S. M., and Koutsoyiannis, D.: Battle of extreme value distributions: A global  
557 survey on extreme daily rainfall, *Water Resources Research*, 49, 187-201, 2013.
- 558 Papalexiou, S. M., and Koutsoyiannis, D.: A global survey on the seasonal variation of  
559 the marginal distribution of daily precipitation, *Advances in Water Resources*, 94, 131-  
560 145, 2016.
- 561 Park, J.-S., and Jung, H.-S.: Modelling Korean extreme rainfall using a Kappa  
562 distribution and maximum likelihood estimate, *Theoretical and Applied climatology*, 72,  
563 55-64, 2002.
- 564 Pilon, P. J., Adamowski, K., and Alila, Y.: Regional analysis of annual maxima  
565 precipitation using L-moments, *Atmospheric Research*, 27, 81-92, 1991.
- 566 Shoji, T., and Kitaura, H.: Statistical and geostatistical analysis of rainfall in central Japan,  
567 *Computers & Geosciences*, 32, 1007-1024, 2006.
- 568 Srikanthan, R., and McMahon, T.: Stochastic generation of annual, monthly and daily  
569 climate data: A review, *Hydrology and Earth System Sciences Discussions*, 5, 653-670,  
570 2001.
- 571 Stedinger, J. R., R.M. Vogel and E. Foufoula-Georgiou: Frequency analysis of extreme  
572 events, *Handbook of Hydrology*, Chapter 18, McGraw Hill Book Co, D.R. Maidment -  
573 editor in chief, 1993..
- 574 Thom, H. C.: A frequency distribution for precipitation, *Bulletin of the American*  
575 *Meteorological Society*, 32, 397, 1951.
- 576 Trenberth, K. E.: Changes in precipitation with climate change, *Climate Research*, 47,  
577 123-138, 2011.
- 578 Vogel, R. M., and Fennessey, N. M.: L moment diagrams should replace product moment  
579 diagrams, *Water Resources Research*, 29, 1745-1752, 1993.
- 580 Vogel, R. W., and McMartin, D. E.: Probability Plot Goodness-of-Fit and Skewness  
581 Estimation Procedures for the Pearson Type 3 Distribution, *Water resources research*, 27,  
582 3149-3158, 1991.
- 583 Waggoner, P.E., 1989: Anticipating the frequency distribution of precipitation if climate  
584 change alters its mean, *Agricultural and Forest Meteorology*, 47, 321 – 337.
- 585 Watterson, I., and Dix, M.: Simulated changes due to global warming in daily  
586 precipitation means and extremes and their interpretation using the gamma distribution,  
587 *Journal of Geophysical Research: Atmospheres*, 108, 2003.



- 588 Watterson, I. G.: Simulated changes due to global warming in the variability of  
589 precipitation, and their interpretation using a gamma-distributed stochastic model,  
590 *Advances in Water Resources*, 28, 1368-1381, 2005.
- 591 Waymire, E., and Gupta, V. K.: The mathematical structure of rainfall representations: 1.  
592 A review of the stochastic rainfall models, *Water resources research*, 17, 1261-1272,  
593 1981.
- 594 Wilby, R. L., and Wigley, T.: Future changes in the distribution of daily precipitation  
595 totals across North America, *Geophysical Research Letters*, 29, 2002.
- 596 Wilks, D. S.: Maximum likelihood estimation for the gamma distribution using data  
597 containing zeros, *Journal of Climate*, 3, 1495-1501, 1990.
- 598 Wilks, D. S.: Multisite generalization of a daily stochastic precipitation generation model,  
599 *Journal of Hydrology*, 210, 178-191, 1998.
- 600 Wilks, D. S., and Wilby, R. L.: The weather generation game: a review of stochastic  
601 weather models, *Progress in physical geography*, 23, 329-357, 1999.
- 602 Woolhiser, D. A., and Roldan, J.: Stochastic daily precipitation models: 2. A comparison  
603 of distributions of amounts, *Water resources research*, 18, 1461-1468, 1982.
- 604 Yoo, C., Jung, K. S., and Kim, T. W.: Rainfall frequency analysis using a mixed Gamma  
605 distribution: evaluation of the global warming effect on daily rainfall, *Hydrological  
606 Processes*, 19, 3851-3861, 2005.

607

608

### 609 **Table captions:**

610 **Table 1:** Review of literature pertinent to daily precipitation probability distribution  
611 selection.

612 **Table 2:** Table 2: Theoretical probability distributions presented on the L-Kurtosis vs L-  
613 Skew L-moment diagram. *Italicized distributions are special cases of other distributions.*

614 **Table 3:** Theoretical probability distributions presented on the L-Cv vs L-Skew L-  
615 moment diagram.

616 **Table 4:** Distributions used in probability plot goodness of fit evaluations.

617 **Table 5:** Central tendency and spread of values of PPCC for the 237 precipitation  
618 stations.

619 **Table 6:** Central tendency and spread of values of PPCC for the 305 areal average  
620 precipitation catchments.

### 621 **Figure captions:**

622 **Figure 1:** Map showing locations of a) 237 precipitation gaging stations, and b) 305  
623 catchments.

624 **Figure 2:** Distribution of full record length of point precipitation base on weather stations.



625 **Figure 3:** Distribution of wet-day record length: a) point precipitation; and b) areal  
626 average precipitation over watersheds. Days with zero precipitation are removed in the  
627 wet-day records

628 **Figure 4:** L-Cv vs L-Skew L-moment ratio diagram of sample L-moments and  
629 theoretical distributions: a) point precipitation; and b) areal average precipitation depths.

630 **Figure 5:** L-Skew vs L-Kurtosis L-moment ratio diagram of sample L-moments and  
631 theoretical distributions: a) point precipitation; and b) areal average precipitation depths.  
632 Logistic (L), Normal (N), Uniform (U), Gumbel (G), and Exponential (E) distributions  
633 appear as a single point.

634 **Figure 6:** Standard boxplots of  $r$  for all 7 distributions evaluated for a) full record, and b)  
635 wet-day series of point precipitation depths.

636 **Figure 7:** Standard boxplots of  $r$  for all 7 distributions evaluated for a) full- record, and b)  
637 wet-day series of areal average precipitation depths.

638 **Figure 8:** Comparison of PPCC ( $r$ ) values for the P3 (vertical axis) and G2 (horizontal  
639 axis) distributions for the a) point precipitation depths' full -record, b) point precipitation  
640 depths' wet-day, c) areal average precipitation depths' full-record, and d) areal average  
641 precipitation depths' wet-day series. Points lying above the line represent stations with a  
642 higher  $r$  for the P3 distribution than G2 distribution.

643 **Figure 9:** Comparison of  $r$  values for P3 (horizontal axis) and KAP (vertical axis)  
644 distributions for the a) point precipitation depths' full-record, b) point precipitation  
645 depths' wet-day, c) areal average precipitation depths' full-record, and d) areal average  
646 precipitation depths' wet-day series.

## 647 **Tables**

648





**Table 1:** Review of literature pertinent to daily precipitation probability distribution selection.

1. Stochastic Precipitation Modelling:						
Author	Year	Stations	Series type	Duration	Distribution	Justification
Thom	1951		Wet-day	1-day	Gamma	
Buishand	1978	6	Wet-day	1-day	Gamma	Cv-Cs ratio
Geng et al	1986	6	Wet-day, by month	1-day, monthly	Gamma	Regress. fit: $\beta$ vs mean wet-day depth
Woolhiser and Roldan	1982		Wet-day	1-day	Mixed Exponential	MLE, Akaike Information Criterion
Duan et al	1995	1	Wet-day, by month	1-day	Calib. W2, Gamma	MLE, Chi-sq test
Wilks	1998	25	Wet-day	1-day	Mixed Exponential	MLE, goodness of fit
Waterson and Dix	2003		Wet-day	1-day	Gamma	Literature
Burgueno et al	2005	75	Wet-day	1-day	Exponential, Weibull	Normalized Rainfall Curve
Waterson	2005		Wet-day	1-day	Gamma	Literature
2. Precipitation Frequency Analysis						
Author	Year	Stations	Series type	Duration	Distribution	Justification
Hershfield (TP-40)	1962		AMS	24 hour	Gumbel	
Pilon et al	1991	75	AMS	5 min - 24 hour	GEV	L-moments
Naghavi & Yu	1995	25	AMS	1-24 hour	GEV	L-moments, PWMs, Monte Carlo experiments
Park and Jung	2002	61	AMS	1, 2-day	Kappa(4)	
Lee and Maeng	2003	38	AMS	1-day	GEV, GLO	L-moments
Bonnin et al	2006		AMS	5 min - 24 hour	GEV	L-moments
Shoji and Kitaura	2006	243	Complete, Wet-day	Hour, Day, Month, Year	Lognormal, Weibull	Goodness of fit
Deidda and Puliga	2006	200	Left Censored Wet-day	1-day	Generalized Pareto	"Failure-to-reject" method, L-moments
Papalexiou and Koutsoyiannis	2012	11,519	Wet-Day	1-day	Generalized Gamma	L-moments
Papalexiou and Koutsoyiannis	2013	15,137	AMS	1-day	GEV	L-moments
Papalexiou and Koutsoyiannis,	2016	14,157	Wet-Day, by month	1-day	Generalized Gamma and Burr type XII	L-moments and Goodness-of-fit
3. Precipitation Trends and Climate Change						
Author	Year	Stations	Series type	Duration	Distribution	Justification
Waggoner	1989	55	Monthly	1-month	Gamma	Literature Review
Groisman et al	1999	1313	Summer (wet-day)	1-day	Gamma	Literature Review, goodness of fit to



							extreme rainfall quantiles
Wilby and Wigley	2002	GCM	Seasonal	1-day	Gamma		Literature Review
Yoo et al	2005	31	Monthly (wet-day)	1-day	Gamma		Literature Review
Watterson	2005	GCM	January, July	1-month (daily forced)	Gamma		Literature Review



**Table 2:** Theoretical probability distributions presented on the L-Kurtosis vs L-Skew L-moment diagram. *Italicized distributions are special cases of other distributions.*

Distribution	Abbreviation	Parameters
Generalized Extreme Value Type III	GEV	3
Generalized Logistic	GLO	3
Generalized Pareto	GPA	3
Lognormal	LN3	3
Pearson Type III	P3	3
<i>Exponential</i>	E	2
<i>Gumbel</i>	G	2
<i>Normal</i>	N	2
<i>Logistic</i>	L	2
<i>Uniform</i>	U	1

**Table 3:** Theoretical probability distributions presented on the L-Cv vs L-Skew L-moment diagram.

Distribution	Abbreviation	Parameters
Gamma	G2	2
Generalized Pareto	GP2	2
Lognormal	LN2	2
Weibull	W2	2

**Table 4:** Distributions used in probability plot goodness of fit evaluations.

Distribution	Abbreviation	Parameters
Generalized Extreme Value Type III	GEV	3
Generalized Logistic	GLO	3
Generalized Pareto	GPA	3
Lognormal	LN3	3
Pearson Type III	P3	3
Gamma	G2	2
Kappa	KAP	4

**Table 5:** Central tendency and spread of values of PPCC for the 237 precipitation stations.

Distribution	Full Record			Percentiles		Wet Day			Percentiles	
	Mean	Median	§	95th	5th	Mean	Median	§	95th	5th
P3	<b>0.9953</b>	<b>0.9962</b>	<b>0.0045</b>	<b>0.9991</b>	<b>0.9892</b>	0.9952	0.9971	0.0063	0.9995	0.9872
GEV	0.5949	0.5928	0.0527	0.6755	0.5166	0.9338	0.9375	0.0222	0.9609	0.8944
GPA	0.6192	0.6177	0.0604	0.7145	0.5339	0.9793	0.9828	0.0145	0.9949	0.9500
GLO	0.5939	0.5922	0.0509	0.6708	0.5172	0.9115	0.9154	0.0235	0.9423	0.8734
LN3	0.7975	0.8078	0.0545	0.8731	0.7055	0.9838	0.9855	0.0075	0.9924	0.9727
G2	0.9945	0.9954	0.0046	0.9988	0.9876	0.9925	0.9949	0.0079	0.9990	0.9789
KAP	0.9780	0.9784	0.0137	0.9926	0.9644	<b>0.9971</b>	<b>0.9985</b>	<b>0.0048</b>	<b>0.9997</b>	<b>0.9915</b>



**Table 6:** Central tendency and spread of values of PPCC for the 305 areal average precipitation catchments.

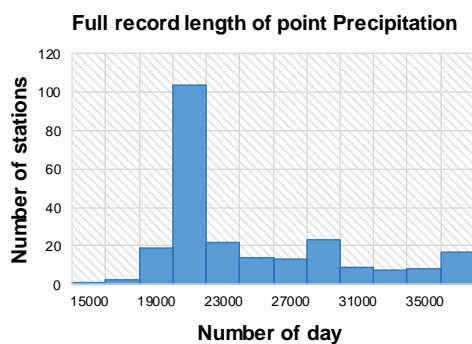
Distribution	Full Record			Percentiles		Wet Day			Percentiles	
	Mean	Median	§	95th	5th	Mean	Median	§	95th	5th
P3	<b>0.9972</b>	<b>0.9975</b>	<b>0.0023</b>	0.9993	<b>0.9941</b>	<b>0.9977</b>	0.9985	<b>0.0028</b>	0.9996	<b>0.9936</b>
GEV	0.6757	0.6706	0.0666	0.8014	0.5836	0.8003	0.7965	0.0474	0.8917	0.7264
GPA	0.7247	0.7177	0.0795	0.8711	0.6140	0.8688	0.8687	0.0484	0.9586	0.7894
GLO	0.6654	0.6607	0.0608	0.7772	0.5803	0.7800	0.7750	0.0441	0.8669	0.7101
LN3	0.8717	0.8736	0.0444	0.9409	0.8035	0.9362	0.9373	0.0224	0.9737	0.8983
G2	0.9967	0.9971	0.0024	0.9992	0.9935	0.9974	0.9985	0.0034	0.9996	0.9924
KAP	0.9959	0.9968	0.0034	<b>0.9996</b>	0.9898	0.9976	<b>0.9987</b>	0.0026	<b>0.9998</b>	0.9929



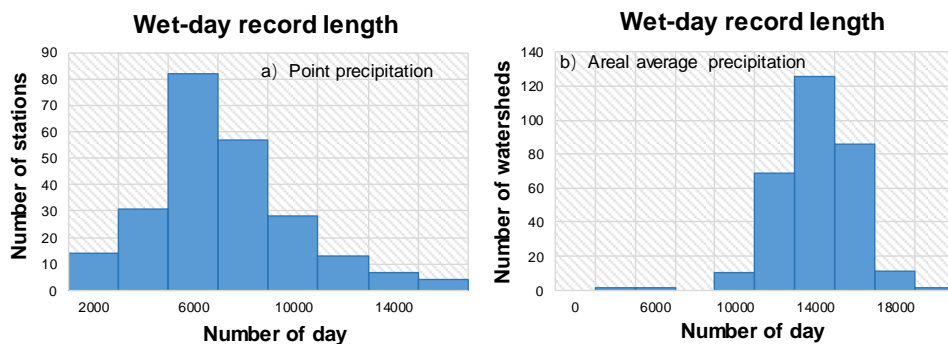
## Figures



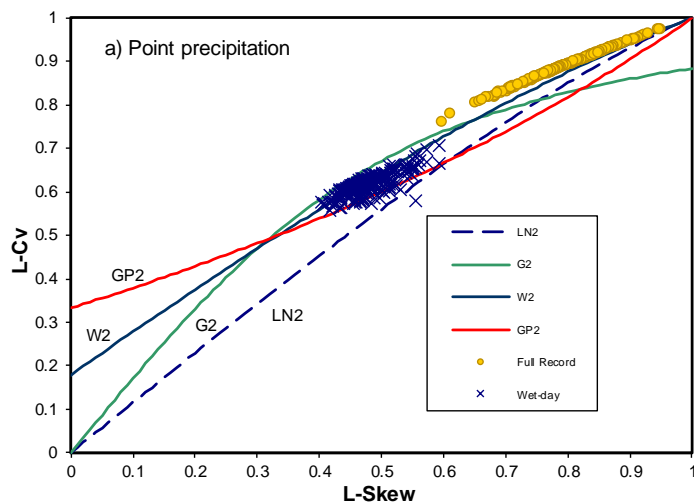
**Figure 1:** Map showing locations of a) 237 point precipitation gaging stations, and b) 305 MOPEX catchments.

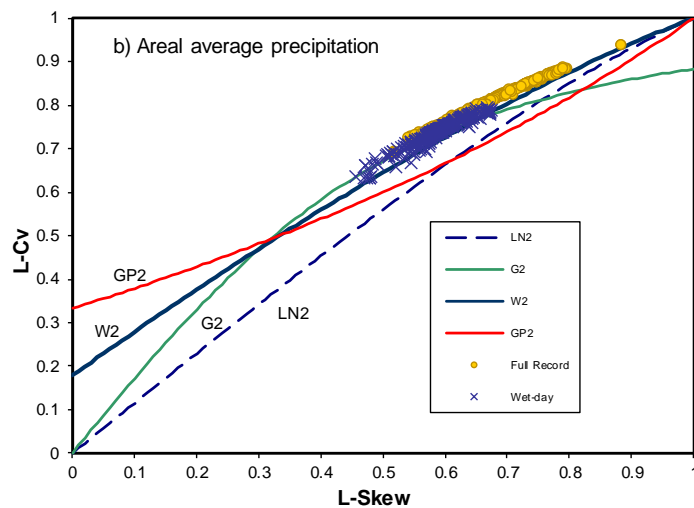


**Figure 2:** Distribution of length of records of point daily precipitation data for the 237 gaging stations depicted in Figure 1a.

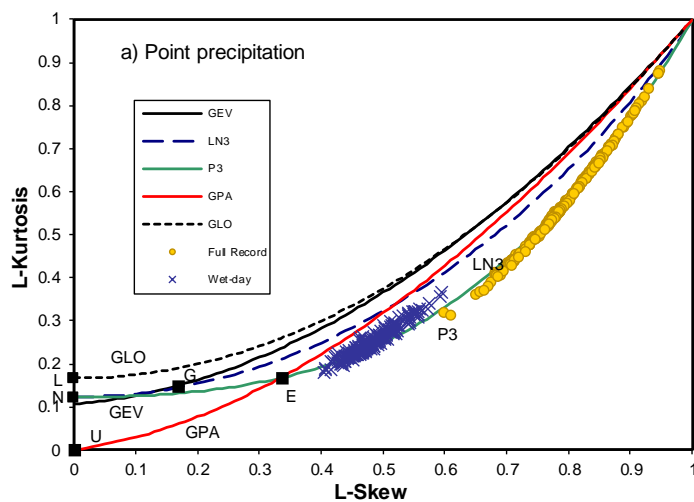


**Figure 3:** Distribution of wet-day record lengths corresponding to the two datasets: a) point precipitation; and b) areal average precipitation over catchments. Days with zero precipitation are removed in the wet-day records





**Figure 4:** L-Cv vs L-Skew L-moment ratio diagram of sample L-moments and theoretical distributions for: a) point daily precipitation; and b) areal average daily precipitation depths.



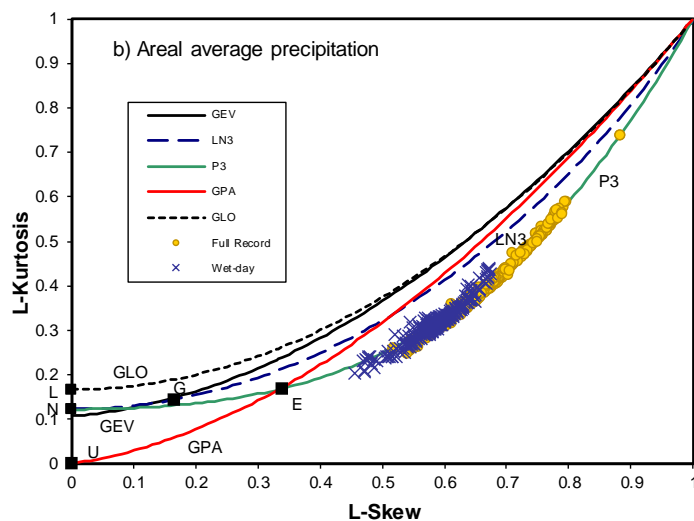


**Figure 5:** L-Skew vs L-Kurtosis L-moment ratio diagram of sample L-moments and theoretical distributions for: a) point daily precipitation; and b) areal average daily precipitation depths. Note that Logistic (L), Normal (N), Uniform (U), Gumbel (G), and Exponential (E) distributions appear as a single point.



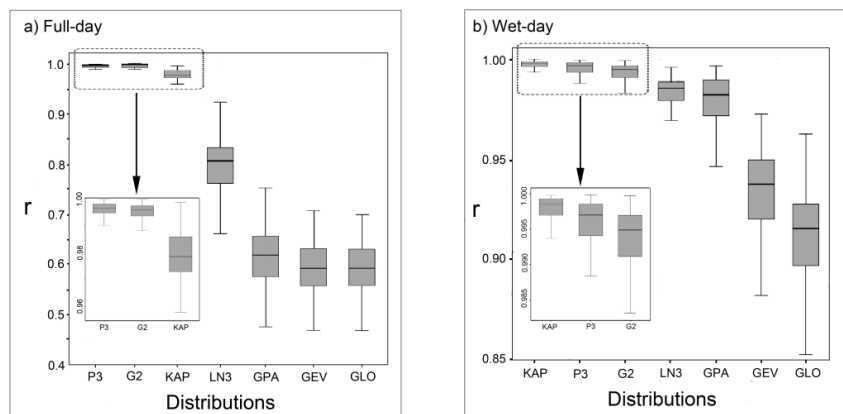


**Figure 6:** Standard boxplots of  $r$  for all 7 distributions evaluated for a) full record, and b) wet-day series of point precipitation depths.

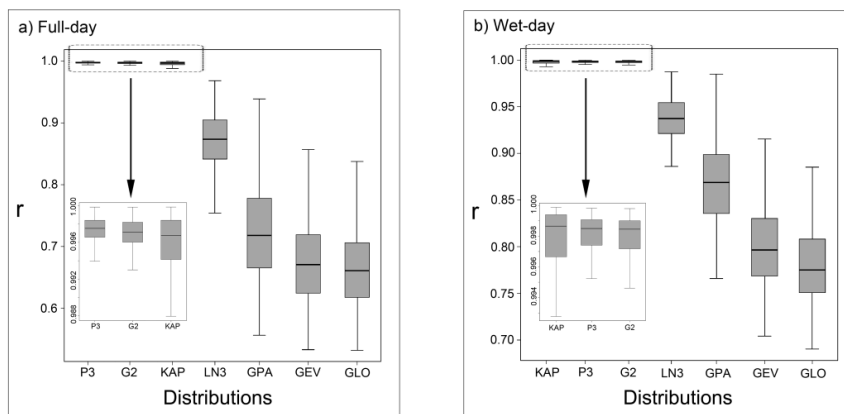


**Figure 7:** Standard boxplots of  $r$  for all 7 distributions evaluated for a) full-record, and b) wet-day series of areal average precipitation depths.

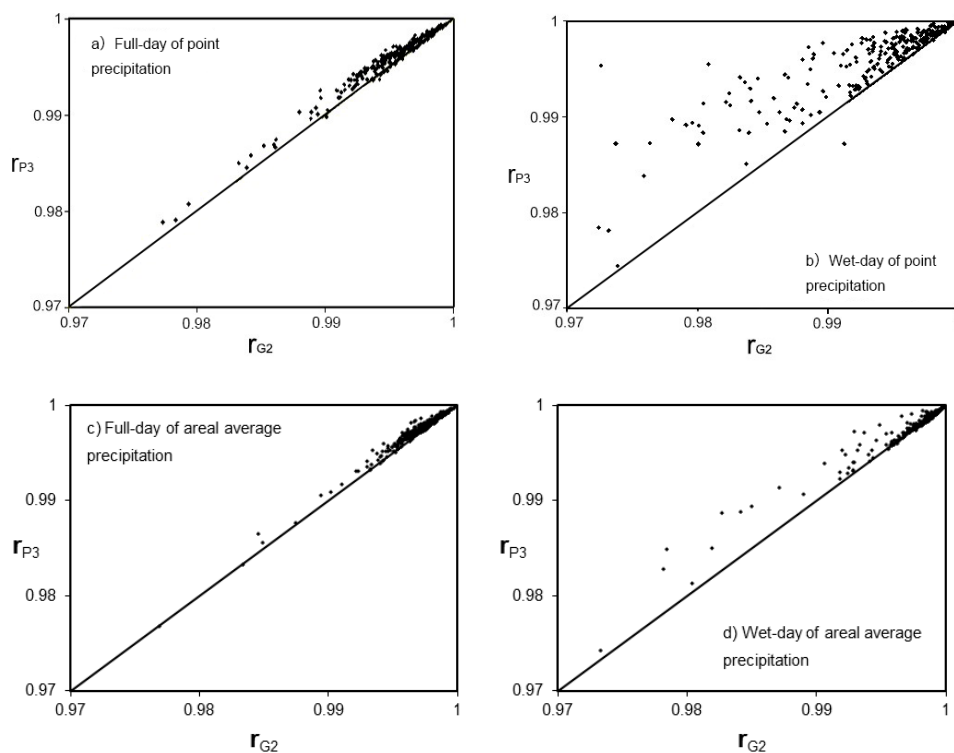


**Figure 8:** Comparison of PPCC ( $r$ ) values for the P3 (vertical axis) and G2 (horizontal axis) distributions for the a) point precipitation depths' full -record, b) point precipitation depths' wet-day, c) areal average precipitation depths' full-record, and d) areal average precipitation depths' wet-day series. Points lying above the line represent stations with a higher  $r$  for the P3 distribution than G2 distribution.

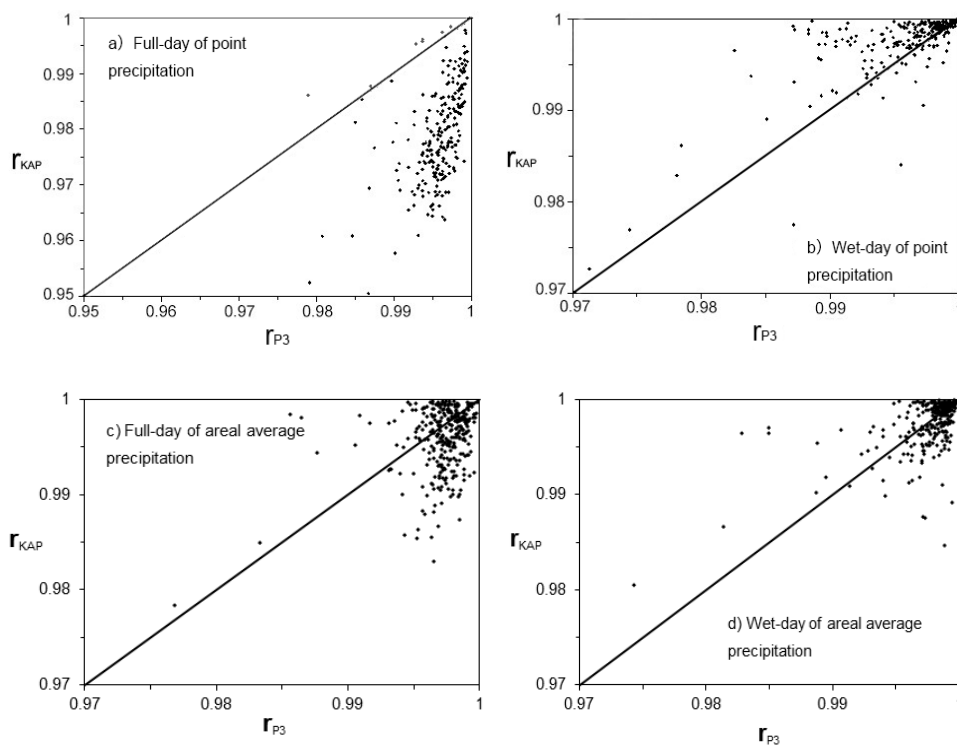


**Figure 9:** Comparison of  $r$  values for P3 (horizontal axis) and KAP (vertical axis) distributions for the a) point precipitation depths' full-record, b) point precipitation depths' wet-day, c) areal average precipitation depths' full-record, and d) areal average precipitation depths' wet-day series.